

$e^+e^- \rightarrow \gamma + \text{missing neutrals: Neutrino versus photino production}$

L. Bento, J. C. Romão, and A. Barroso

CFN/CFMC, Universidades de Lisboa, Av. Gama Pinto 2, 1699 Lisboa, Portugal

(Received 29 July 1985)

We have calculated the cross sections for the processes $e^+e^- \rightarrow \gamma\nu\bar{\nu}$ and $e^+e^- \rightarrow \gamma\tilde{\gamma}\tilde{\gamma}$. The local-limit approximation for the W -exchange diagram was not used and the integration over the neutrino and photino phase space was done analytically. The use of polarized beams is discussed as a way to improve the signal-to-background ratio of the supersymmetric process.

At present, there is great interest in the study of spontaneously broken supersymmetric gauge models (see Refs. 1 and 2 for recent reviews). In several of these models the photino $\tilde{\gamma}$ is the lightest supersymmetric particle. Hence it was suggested early³ that the search for the reaction $e^+e^- \rightarrow \gamma\tilde{\gamma}\tilde{\gamma}$ could provide a useful supersymmetry (SUSY) signature. Since then other authors⁴⁻⁶ have calculated the exact cross section for this process using finite photino and scalar-electron masses. On the other hand, there are already some preliminary experimental results,⁷ and with improved sensitivity and running time these experiments will give important limits on $m_{\tilde{e}}$ and $m_{\tilde{\gamma}}$.

Clearly, the observation of the reaction $e^+e^- \rightarrow \gamma X$, where X is invisible, does not imply the existence of photinos. More likely, X is a neutrino-antineutrino pair, and, by measuring the cross section for $e^+e^- \rightarrow \gamma X$, one is counting the number of neutrinos.

However, the observation of a signal above the one predicted by the standard model would certainly require some "new physics." So it is important to calculate accurately the neutrino cross section. Our aim was to calculate this cross section and to compare it with the photino production cross section. Despite the fact that the photino process was studied in three recent publications, we think that it is still useful to write this Brief Report. Rather than du-

plicating the existing work we make this note complementary to the previous papers. The emphasis will be on the new aspects of our calculation, which are the following: (i) the evaluation of the neutrino cross section without the previously used 4-point approximation for the W -exchange diagram, (ii) the exact analytic integration over the neutrino and photino phase space, and (iii) the discussion of the use of polarized beams as a way to improve the signal-to-background ratio of the SUSY process.

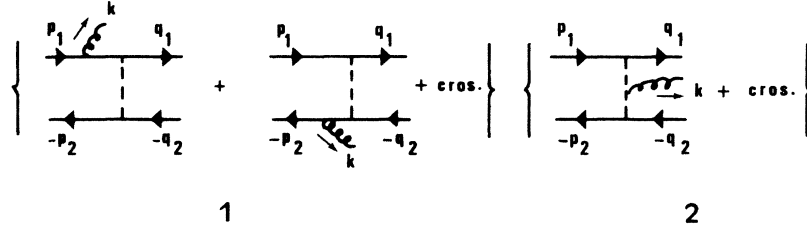
First, let us consider the neutrino production cross section. We denote by p_1 (p_2) the momentum of the incoming electron (positron), by q_1 (q_2) the momentum of the neutrino (antineutrino), and by k the photon momentum.

After integrating over the neutrino phase space one obtains the differential cross section $d\sigma/dx dy$, where x is the photon energy in units of the beam energy ($\sqrt{s}/2$) and $y = \cos\theta$, with θ the angle between k and p_1 . We have

$$\frac{d\sigma}{dx dy} = \sum_{i,j} \frac{d\sigma^{ij}}{dx dy}; \quad i,j = Z, W_1, W_2,$$

where we have split the W -exchange diagrams in two parts; W_1 corresponding to the diagrams where the photon is coupled with the leptons, and W_2 corresponding to the diagram with a $WW\gamma$ coupling. The various contributions are

$$\begin{aligned} \frac{d\sigma^{ZZ}}{dx dy} &= \frac{6CM_Z^4(g_V^2 + g_A^2)}{[(\Delta^2 - M_Z^2)^2 + M_Z^2\Gamma_Z^2]} \{ \hat{I}[-\Delta \cdot p_1 p_1 \cdot q_1 k \cdot q_2 + k \cdot p_1 p_2 \cdot q_1 p_2 \cdot q_2 + \frac{1}{2}(s - \Delta \cdot k)p_1 \cdot q_2 p_2 \cdot q_1] + (1 \leftrightarrow 2) \}, \\ \frac{d\sigma^{ZW_1}}{dx dy} &= \frac{CM_W^2 M_Z^2 (g_V + g_A)(\Delta^2 - M_Z^2)}{[(\Delta^2 - M_Z^2)^2 + M_Z^2\Gamma_Z^2]} \{ \hat{I}_{22}[-4k \cdot p_2 p_2 \cdot q_1 k \cdot q_2 + [(\Delta \cdot k - s)p_1 \cdot q_2 p_2 \cdot q_1 - 2k \cdot p_1 p_2 \cdot q_1 p_2 \cdot q_2 \\ &\quad + sp_1 \cdot q_2 k \cdot q_1 + (1 \leftrightarrow 2)]] + (1 \leftrightarrow 2) \}, \\ \frac{d\sigma^{ZW_2}}{dx dy} &= \frac{-2CM_W^2 M_Z^2 (g_V + g_A)(\Delta^2 - M_Z^2)}{[(\Delta^2 - M_Z^2)^2 + M_Z^2\Gamma_Z^2]} \{ k \cdot p_2 \hat{I}_{11,22}[2p_1 \cdot q_2 p_2 \cdot q_1(2p_1 \cdot q_1 - k \cdot q_1) + 2p_1 \cdot q_1(k \cdot p_2 p_1 \cdot q_2 - p_2 \cdot q_1 k \cdot q_2) \\ &\quad - sp_1 \cdot q_2 k \cdot q_1 + k \cdot p_1 p_2 \cdot q_1(4k \cdot q_2 + \Delta^2)] + (1 \leftrightarrow 2) \}, \\ \frac{d\sigma^{W_1 W_1}}{dx dy} &= 4CM_W^4 \{ k \cdot p_2 \hat{I}_{22,22}[p_2 \cdot q_1 k \cdot q_2] + k \cdot p_1 \hat{I}_{11,11}[p_1 \cdot q_2 k \cdot q_1] \\ &\quad + \hat{I}_{11,22}[\frac{1}{4}s(\Delta^2 - 2p_1 \cdot q_1)p_1 \cdot q_2 + k \cdot p_1 p_2 \cdot q_1(p_2 \cdot q_2 - p_1 \cdot q_2)] + (1 \leftrightarrow 2) \}, \\ \frac{d\sigma^{W_1 W_2}}{dx dy} &= 4CM_W^4 \{ k \cdot p_2 \hat{I}_{11,22,22}[2p_1 \cdot q_2 p_2 \cdot q_1(2p_1 \cdot q_1 - k \cdot q_1) + 2p_1 \cdot q_1(k \cdot p_2 p_1 \cdot q_2 - p_2 \cdot q_1 k \cdot q_2) \\ &\quad - sp_1 \cdot q_2 k \cdot q_1 + k \cdot p_1 p_2 \cdot q_1(4k \cdot q_2 + \Delta^2)] + (1 \leftrightarrow 2) \}, \\ \frac{d\sigma^{W_2 W_2}}{dx dy} &= 4CM_W^4 k \cdot p_1 k \cdot p_2 \{ \hat{I}_{11,11,22,22}[2p_1 \cdot q_1 p_2 \cdot q_1(2p_1 \cdot q_2 - k \cdot q_2) + 2k \cdot p_1 p_2 \cdot q_1 p_2 \cdot q_2 \\ &\quad + (4k \cdot p_1 - s)p_2 \cdot q_1 k \cdot q_2 + \Delta^2 k \cdot p_1 p_2 \cdot q_1] + (1 \leftrightarrow 2) \}, \end{aligned} \quad (1)$$

FIG. 1. Feynman diagrams for the process $e^+e^- \rightarrow \tilde{\gamma}\tilde{\gamma}\gamma$.

where

$$C = 2G_F^2 \alpha / [\pi^3 s^2 x (1 - y^2 + 4m_e^2 y^2 / s)] ,$$

$$\Delta = p_1 + p_2 - k ,$$

and for each argument $f(q_1, q_2)$ we have

$$\hat{I}_{ij,lm} \dots [f(q_1, q_2)] = \int \frac{d^3 q_1}{2E_1} \frac{d^3 q_2}{2E_2} \frac{\delta^4(q_1 + q_2 - \Delta)}{N_{ij} N_{lm} \dots} f(q_1, q_2) ,$$

with

$$N_{ij} = M_W^2 - (p_i - q_j)^2 \quad i, j = 1, 2 .$$

$$\begin{aligned} \frac{d\sigma^{11}}{dx dy} = & \tilde{C} \{ (2k \cdot p_2 \hat{I}_{22,22} [p_2 \cdot q_2 k \cdot q_1] - m_{\tilde{\gamma}}^2 (k \cdot p_2)^2 I_{22,21} + (1 \leftrightarrow 2)) - \frac{1}{2} m_{\tilde{\gamma}}^2 s \Delta^2 I_{11,21} \} \\ & + \tilde{C} \{ \hat{I}_{11,22} [(s - \Delta \cdot k) p_1 \cdot q_1 p_2 \cdot q_2 - s p_2 \cdot q_2 k \cdot q_1 + 2k \cdot p_1 p_2 \cdot q_1 p_2 \cdot q_2] + (1 \leftrightarrow 2) \} , \end{aligned}$$

$$\frac{d\sigma^{22}}{dx dy} = 2\tilde{C} k \cdot p_1 k \cdot p_2 \{ 4\hat{I}_{11,11,22,22} [p_1 \cdot q_1 p_2 \cdot q_2 (p_1 \cdot q_1 + p_2 \cdot q_2)] - s m_{\tilde{\gamma}}^4 I_{11,12,21,22} \} , \quad (2)$$

$$\begin{aligned} \frac{d\sigma^{12}}{dx dy} = & \tilde{C} \{ 4k \cdot p_2 \hat{I}_{11,22,22} [p_2 \cdot q_2 (p_1 \cdot q_1 (\Delta^2 - 2p_2 \cdot q_2 + k \cdot q_1) + m_{\tilde{\gamma}}^2 k \cdot p_1)] \\ & - m_{\tilde{\gamma}}^2 k \cdot p_2 \hat{I}_{12,21,22} [2(s - k \cdot p_2) p_1 \cdot q_2 + s(k \cdot p_1 - k \cdot q_2) + 2k \cdot p_1 p_2 \cdot q_2] + (1 \leftrightarrow 2) \} , \end{aligned}$$

where

$$\tilde{C} = 16\alpha^3 / [\pi s^2 x (1 - y^2 + 4m_e^2 y^2 / s)] ,$$

and

$$I_{ij} \dots = \hat{I}_{ij} \dots [f(q_1, q_2) = 1] ,$$

Notice that we have consistently neglected the electron mass and considered the approximation of degenerate scalar-electron masses.

Our results are shown in Figs. 2-4. In Fig. 2 we plot the total cross sections $\sigma(\nu\bar{\nu}\gamma)$ and $\sigma(\tilde{\gamma}\tilde{\gamma}\gamma)$ for $m_{\tilde{\gamma}} = 5 \text{ GeV}/c^2$ and $m_e = 40 \text{ GeV}/c^2$ using the cuts $|y| \leq 0.94$ and $0.2 \leq x \leq 1$. As far as one can judge, comparing our curves with the corresponding ones published by Grassie and Pandita,⁵ the agreement is very good. Our photino cross section is twice as big as theirs because we sum the contributions of the two degenerate scalar electrons. The comparison with the other two calculations is not so easy and we noticed several misprints in the square of the invariant matrix elements listed in Ref. 6. Even for $\sigma(\nu\bar{\nu}\gamma)$ the agreement with Ref. 5 is good despite the fact that the authors used the local-limit approximation. In fact, for $\sqrt{s} = 100 \text{ GeV}$, this approximation overestimates the W contribution by a factor of 1.2. But the effect on the total cross section is marginal, of the order of 2%, due to the overwhelming contribution of the Z diagram. Clearly, this is not true if we calculate $d\sigma/dx dy$ far from the resonance. For instance,

A similar integral without the denominators, N_{ij}, \dots , defines $\hat{I}[f(q_1, q_2)]$. Details of these integrations can be found elsewhere⁸ and the values of the integrals are listed in the Appendix.

The mass and width of the Z boson are denoted M_Z and Γ_Z , respectively, and in the numerical evaluation we have used $M_Z = 92 \text{ GeV}/c^2$, $\Gamma_Z = 2.8 \text{ GeV}/c^2$, $g_A = -\frac{1}{2}$, and $g_V = -\frac{1}{2} + 2 \sin^2 \theta_W$, with $\sin^2 \theta_W = 0.215$.

For the photino reaction the amplitude is given by the diagrams of Fig. 1; with a similar kinematics and an obvious notation we obtain

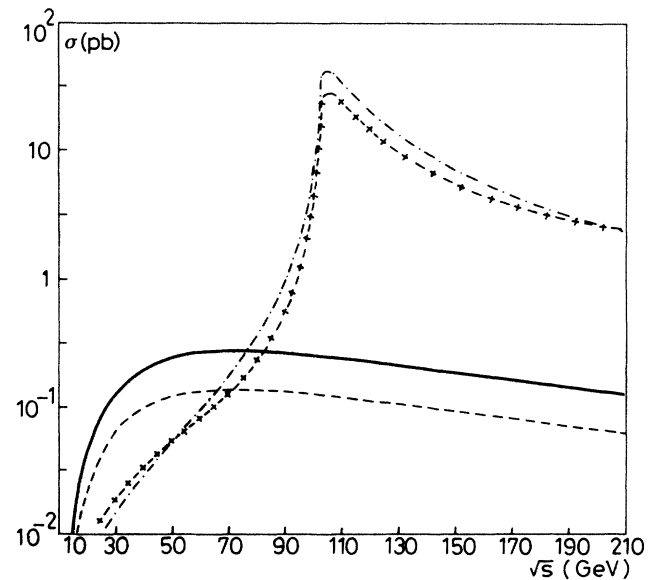


FIG. 2. Photino cross section as a function of \sqrt{s} for unpolarized (dashed curve) and polarized (solid curve) beams. The dashed-crossed and dashed-dotted curves are the neutrino cross section for unpolarized and polarized beam, respectively.

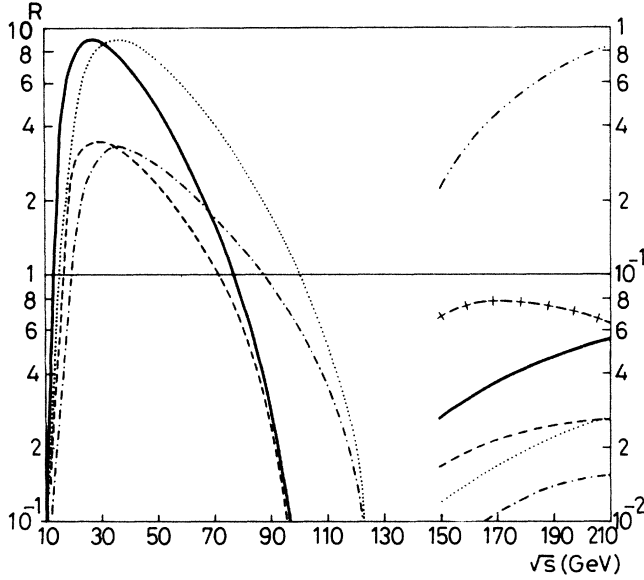


FIG. 3. R as a function of \sqrt{s} . The different curves have the following meaning: dashed, unpolarized $x \geq 0.2$; solid, polarized $x \geq 0.2$; dashed-dotted, unpolarized $x \geq 0.5$; dotted, polarized $x \geq 0.5$; dashed-crossed, unpolarized $0.2 \leq x \leq 0.5$; dashed-double-dotted, polarized $0.2 \leq x \leq 0.5$.

for $\sqrt{s} = 200$ GeV and $0.2 \leq x \leq 0.5$ the local approximation overestimates σ by a factor of 2.1.

The large- Z contribution to the neutrino cross section completely washes away any signal of photino production for $\sqrt{s} \geq 80, 90$ GeV. This feature is clearly seen in Fig. 3, where we show the ratio $R = \sigma(\tilde{\gamma}\tilde{\gamma}\gamma)/\sigma(\nu\bar{\nu}\gamma)$. The dashed curve represents R for the same kinematic cuts and the same $m_{\tilde{e}}$ and $m_{\tilde{\gamma}}$. R is maximum for $\sqrt{s} = 30$ GeV and drops below 0.5 for $\sqrt{s} \geq 80$ GeV. For small energies R decreases when $\sqrt{s} \rightarrow 0$ because the photinos are massive while the neutrinos are massless.

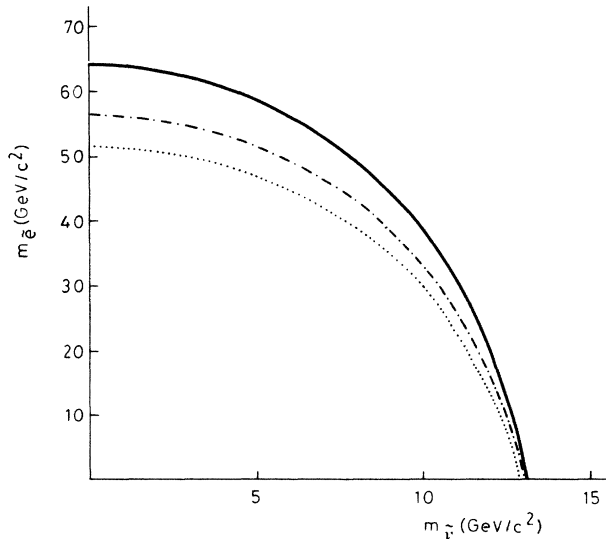


FIG. 4. Discovery limits corresponding to $\sqrt{s} = 30$ GeV and $L_i = 100$ pb $^{-1}$. Dotted curve, unpolarized; dot-dashed, e_R^- ; solid, $e_R^+ e_L^+$.

Trying to increase R we were led to study the same reactions with polarized beams. At high energy there are effectively two polarization channels $e_L^- e_R^+$ and $e_R^- e_L^+$. They both contribute equally to the photino production, but the RL channel gives the minimum contribution to the neutrinos background process. The full curve in Fig. 3 represents R for RL polarized beams, using again the same values of y , x , $m_{\tilde{e}}$, and $m_{\tilde{\gamma}}$. The other two curves display the comparison between unpolarized and RL polarized values of R for a higher cut in x ($x \geq 0.5$). In all cases the use of polarized beams improves R and for energies above the Z resonance it can amplify R by an order of magnitude. This can be seen on the right-hand side of Fig. 3, where the curves for polarized and unpolarized beams were plotted for $0.2 \leq x \leq 0.5$ (notice the different scale). However, one should keep in mind that in this region R only reaches 0.7 at $\sqrt{s} \approx 200$ GeV. Below M_Z , R can be larger than one and the polarization of the beams enhances R by a factor of 2–3.

In this domain of \sqrt{s} a larger cut in x could be a useful way of extending the region of $R > 1$ towards higher values of \sqrt{s} . Obviously this gain has to be balanced against a reduction in the total number of events. It is worthwhile to point out that the same values of R can be obtained with a R -polarized e^- beam scattering off unpolarized positrons. The polarization of the two beams increases both cross sections by a factor of 2 and so it has no effect on R besides giving better statistics.

Another interesting way of looking at our results is as SUSY discovery limits in the $m_{\tilde{\gamma}} m_{\tilde{e}}$ plane. For this we need some criteria for the minimum R necessary for an experimental separation of the photino and neutrino processes. Since $\sigma(\tilde{\gamma}\tilde{\gamma}\gamma)$ is at most of the order of 10^{-1} pb and a realistic integrated luminosity cannot be larger than 100–200 pb $^{-1}$, the number of events will be small and the statistical error relatively large. Leaving aside a sophisticated statistical analysis we consider, for illustrative purposes, that SUSY would be discovered if

$$T - \sqrt{T} \geq N + \sqrt{N},$$

where N is the predicted number of standard events and T is N plus the predicted number of photino events. In Fig. 4 the area inside the curves corresponds to the values of $m_{\tilde{e}}$ and $m_{\tilde{\gamma}}$ which meet our discovery criteria for a $e^- e^+$ collision with 30-GeV center-of-mass energy. The dotted, dashed-dotted, and full curves refer to unpolarized, R polarized electron, and polarized e_R^-, e_L^+ beams, respectively, assuming an integrated luminosity L_i of 100 pb $^{-1}$. Again, one can see that using polarized leptons increases the chances of discovering SUSY.

APPENDIX

We obtain⁸ the following recurrence relations:

$$\begin{aligned} \hat{I}_{ij,lm,\dots}[p_i \cdot q_k f] \\ = \frac{1}{2} \times \begin{cases} -\delta \hat{I}_{ij,lm,\dots}[f] + \hat{I}_{lm,\dots}[f], & k=j, \\ (2\Delta \cdot p_i + \delta) \hat{I}_{ij,lm,\dots}[f] - \hat{I}_{lm,\dots}[f], & k \neq j, \end{cases} \quad (A1) \end{aligned}$$

$$\hat{I}_{ij,\dots}[k \cdot q_m] = (\Delta \cdot k I_{ij,\dots} + \epsilon_m \hat{I}_{ij,\dots}[k \cdot q])/2, \quad (A2)$$

$$\hat{I}_{ij,\dots}[k \cdot q] = \hat{I}_{ij,\dots}[p_1 \cdot q] + \hat{I}_{ij,\dots}[p_2 \cdot q], \quad (A3)$$

$$\hat{I}_{ij, \dots, ij} [u \cdot q] = \frac{(p_i, u)}{(p_i, p_i)} \epsilon_j \left[I_{ij, \dots, ij} - A_i I_{ij, \dots, ij} \right]_{n \text{ times}}, \quad (\text{A4})$$

$$\hat{I}_{ij', kl', \dots} [u_1 \cdot q u_2 \cdot q \dots u_m \cdot q] = (-1)^m \hat{I}_{ij, kl, \dots} [u_1 \cdot q u_2 \cdot q \dots u_m \cdot q], \quad j' \neq j, \quad l' \neq l, \dots, \quad (\text{A5})$$

with

$$\delta = \begin{cases} M_W^2 - m_e^2, & \text{neutrinos,} \\ m_\pi^2 - m_e^2 - m_\gamma^2, & \text{photinos,} \end{cases}$$

$$\epsilon_m = (-1)^{m+1}, \quad q = q_1 - q_2, \quad A_i = \delta + \Delta \cdot p_i,$$

and u_n denotes any 4-vectors but q_i . For convenience we define the "scalar product" $(a, b) = \Delta \cdot a \Delta \cdot b - \Delta^2 a \cdot b$.

With a judicious use of these relations all integrals $\hat{I}_{ij, \dots} [f]$ in Eqs. (1) and (2) can be expressed in terms of $\hat{I}_{ij, \dots} = \hat{I}_{ij, \dots} [f=1]$. Defining

$$N_{ij} = \begin{cases} M_W^2 - (p_i - q_j)^2, \\ m_\pi^2 - (p_i - q_j)^2, \end{cases} \quad i, j = 1, 2,$$

$$\beta = \begin{cases} 1 \\ (1 - 4m_\gamma^2/\Delta^2)^{1/2} \end{cases},$$

$$B_i = \beta (p_i, p_i)^{1/2},$$

$$A = (A_i - A_k)^2 - \beta^2 (\epsilon_i p_k - \epsilon_j p_i, \epsilon_i p_k - \epsilon_j p_i),$$

$$B = A_i^2 - A_k^2 + \beta^2 [(p_k, p_k) - (p_i, p_i)],$$

$$D = (A_i + A_k)^2 - \beta^2 (\epsilon_j p_i + \epsilon_i p_k, \epsilon_j p_i + \epsilon_i p_k),$$

and

$$R = (B^2 - AD)^{1/2},$$

we obtain

$$I_{ij} = \frac{\beta \pi}{4 B_i} \ln [(A_i + B_i)/(A_i - B_i)],$$

$$I_{ij, kl} = \begin{cases} \frac{\beta \pi}{2} / (A_i^2 - B_i^2), & i = k, j = l, \\ \frac{\beta \pi}{2R} \ln [(D - A + 2R)/(D - A - 2R)], \end{cases}$$

$$I_{11, 11, 22, 22} = -\partial_2 I_{11, 11, 22},$$

$$I_{11, 11, 22} = -\partial_1 I_{11, 22},$$

$$I_{i1, i2, kj} = (I_{i1, kj} + I_{i2, kj}) / (2A_i),$$

$$I_{11, 12, 21, 22} = (I_{11, 21, 22} + I_{12, 21, 22}) / (2A_1),$$

where ∂_i represents the derivative with respect to A_i .

$$I = \beta \pi / 2,$$

$$\hat{I}[u \cdot q] = 0,$$

$$\hat{I}[u \cdot q \nu \cdot q] = \beta^3 \pi (u, \nu) / 6.$$

¹H. P. Nilles, Phys. Rep. **110**, 1 (1984).

²H. E. Haber and G. L. Kane, Phys. Rep. **117**, 75 (1985).

³J. A. Grifols, X. Mor-Mur, and J. Sola, Phys. Lett. **114B**, 35 (1982); P. Fayet, *ibid.* **117B**, 460 (1982); J. Ellis and J. Hagelin, *ibid.* **122B**, 303 (1982).

⁴T. Kobayashi and M. Kuroda, Phys. Lett. **139B**, 208 (1984).

⁵K. Grassie and P. N. Pandita, Phys. Rev. D **30**, 22 (1984).

⁶J. D. Ware and M. E. Machacek, Phys. Lett. **142B**, 300 (1984).

⁷MAC Collaboration, H. R. Band, in *Proceedings of the 1984 Rencontre de Moriond: Electroweak Interactions and Unified Theories, La Plagne, France*, edited by J. Tran Than Van (Editions Frontières, Gif-sur-Yvette, 1984).

⁸L. Bento, M.Sc. thesis, Universidade de Lisboa, 1985.